Generation and Stability of Charged Toroidal Droplets

A Thesis

Presented to

The Academic Faculty

by

Aaron T. Aizenman

In Partial Fulfillment

of the Requirements of the Degree

Bachelor of Science Research Option

School of Physics

Georgia Institute of Technology

Spring 2018

Dedication

To my parents, David and

Teri Aizenman for always giving

me the advice that I need to hear

Acknowledgments

First, I'd like to thank Dr. Alexandros Fragkopoulos, Dr. Perry Smith, and Dr. Alberto Fernandez-Nieves for teaching me everything I know about experimental research. I would also like to thank Jonas Cuadrado and Mike Tennenbaum, both of whom never hesitated to answer any question I may have. Finally, I would like to thank Dr. Peter Yunker for offering constructive feedback through the creation of this document.

Abstract

In this project, we have determined the quantitative parameters governing the transition phases of charged toroidal droplets. An instability reminiscent of the Saffman-Taylor Instability (viscous fingers) has been observed when toroidal droplets are exposed to a significantly high voltage source, but this is the only recorded development of this instability in a three-dimensional situation (Alberto Fernandez-Nieves 2016). We created a silicon oil environment of extremely high viscosity with aminopropyl terminated silicon oil (ATSO) added to lower surface tension. We utilized surfactants to minimize the surface tension between the inner and outer fluids to slow down the dynamics of the system enough to give the surface a chance to reach equipotential, thus allowing us to test the theories that currently exist in the field. In an attempt to disprove the possibility that this was the Saffman-Taylor Instability, we also attempted viscosity inversion experiments. These failed, thus giving us almost conclusive proof that this was indeed the Saffman-Taylor Instability. By proving that this is indeed the Saffman-Taylor Instability, we have also proven that this three-dimensional problem can be analyzed as a series of two-dimensional problems. This approach vastly simplifies further calculations and analysis of similar systems. A secondary focus of this project was to perfect a method of automated generation of inherently unstable shapes in viscoelastic materials. By using a novel method of 3D printing, the project attempted to increase the efficiency with which we can generate samples for testing and observation while also adding uniformity and consistency to the trials and experiments.

TABLE OF CONTENTS

CHAPTER 1

INTRODUCTION

From raindrops falling from the sky to a stream of water from a kitchen sink faucet to standardized manufacturing processes, bubbles and droplets consistently appear in everyday life. They naturally form spheres, and any non-spherical bubble or droplet (i.e. a cylinder or a ring) is inherently unstable due to surface tension [1]. Surface tension is the tendency of a fluid to minimize its surface area for a given volume. This means that a bubble or droplet will always tends to revert to a spherical shape. Bubbles and droplets occur naturally, but sometimes may be indicative of leaks, flaws, or other inefficiencies in a process. For example, enhanced oil extraction uses water to push crude oil through porous rocks, and the water pushes through the oil, developing fingers that eventually form droplets and trap oil underground. This phenomenon is called either viscous fingering or the Saffman-Taylor instability. A deeper understanding of the dynamics of bubbles and droplets will not only help resolve these inefficiencies, but also answer interesting mathematical and physical questions [1].

A thin enough toroidal droplet will evolve similarly to a liquid jet (see Fig. 1.1). That is, the circular cross section exhibits polar symmetry, but the central ring of the toroid develops perturbations, and the toroid eventually pinches into a series of similarly sized

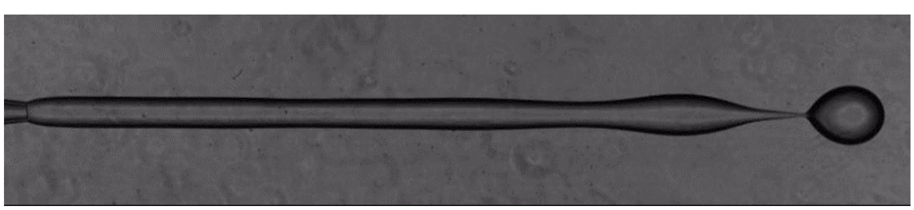

Figure 1.1: A liquid jet. The source of the liquid is on the left, and as time passes, the cylindrical jet develops perturbations and eventually pinches into droplets.

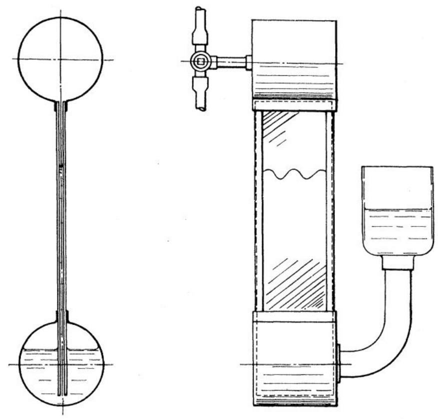

(a) A schematic representation of Saffman and Taylor's experiment. This is a two dimensional cell with a less viscous fluid of high density on top of a more viscous fluid of a lower density.

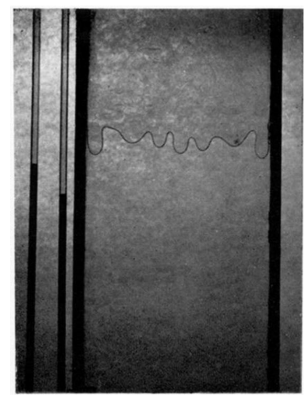

(b) A photo of a live experiment. According to Saffman and Taylor, these fingers are not observed when the upper fluid has a lower viscosity than the fluid on bottom.

Figure 1.2: Saffman and Taylor's Hele-Shaw Cell experiment demonstrating viscous fingering.

droplets [2] Electrified jets have been studied, but only theoretically. The theory covers the regime in which the timescale associated with the electrified flow is very short, yet assumes that the charge has equilibrated on the surface of the jet. By increasing the timescale of the electrified flow, we can study electrified jets that do have an equipotential surface and test the current theory.

We generate toroidal droplets in low surface tension environments to extend the lifespan for as long as possible, and then charge a metallic needle in contact with the droplet, and examine the system as it evolves. Current experiments show that for high enough voltages, electrified toroids do not evolve as neutral jets, but break up via other mechanisms [3]. Instead of pinching into uniform droplets, the toroid expands outwards, and eventually ejects fingers into the outer environment. These are called viscous fingers.

Viscous fingers have only been induced previously by gravitational or mechanical forces, and only seen in two dimensional interfaces or porous media, so seeing these fingers induced by what seems to be electrostatic forces is unexpected given the mechanical properties of the system. The first experimental analysis of these viscous fingers was done by Phillip Saffman and Geoffrey Taylor. They had a two dimensional cell with a viscous fluid underneath a reservoir of a less viscous fluid, and observed the fingers that were developed as a result of gravitational forces, viscosity differences, and density differences. A schematic of their setup and a photo from their results can be seen in Fig 1.2. Additionally, the novel method by which we generate these toroidal droplets has vast implications for the printing of other unstable shapes.

CHAPTER 2

LITERATURE REVIEW

Soft condensed matter is arguably one of the most active research areas of physics now. Governing everything from liquids to polymers to glasses, soft condensed matter is concerned with matter where the spaces between constituent particles is large compared to the particle size. This characteristic leads to mechanically soft materials [1]. Surface phenomena that exist with only insufficient explanation are where our research is focused. Specifically, we are concerned with inherently unstable droplets and their possible stabilization.

One such droplet that we are concerned with is toroidal droplets. Due to surface tension, every droplet tends toward the shape of a sphere, the minimum amount of surface area for a given volume [4]. Given this fact, a toroidal droplet will only exist for a finite amount of time before surface tension take over and the toroid will break. In cylinders, Tomotika examined the case of a cylindrical jet breaking up in a medium of another viscous liquid. As Fragkopoulos showed, when a toroidal droplet has a high enough aspect ratio - that is, the torus is thin enough - any small part of the toroid can be examined as behaving within the cylindrical limit, and the same thread breakup occurs, giving rise to a number of identically sized spherical droplets. However, at lower aspect ratios, the toroid collapses and forms one spherical droplet [2]. See Fig. 2.1.

A question that begs answering is as follows: how can we balance surface tension against another stress to stabilize this unstable liquid droplet? It is certainly possible to generate a toroidal droplet via a rotating stage, as demonstrated by Pairam, but this is always subject to the aforementioned breakup tendencies [5]. It is possible for an unactivated polymer solution, perhaps a solution with Igracure, to be used in the creation

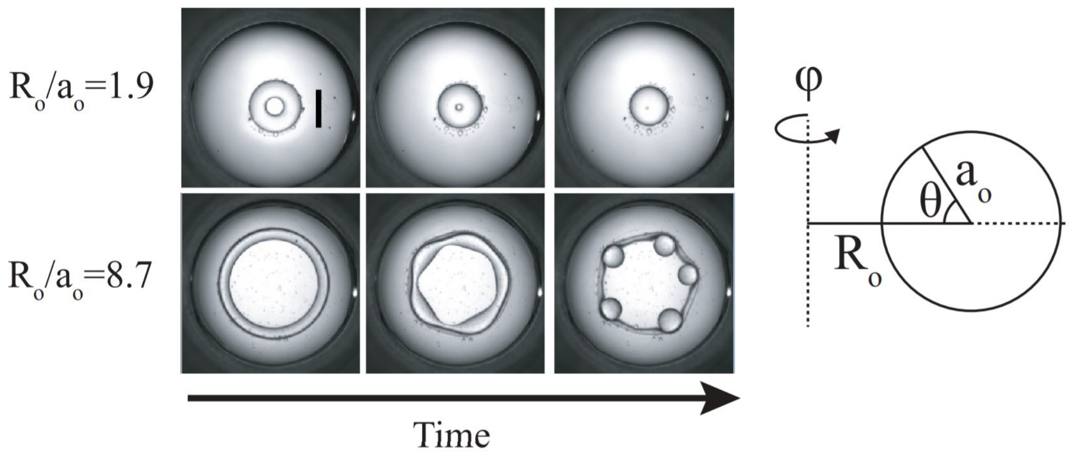

Figure 2.1: Thicker tori (lower aspect ratios) tend to collapse into one sphere containing the entire volume of the droplet. Thinner tori (higher aspect ratios) tend to break into uniformly sized droplets. The aspect ratio is defined as R_0/a_0. R_0 is the radius from the axis of rotation to the center of the tube, a_0 is the radius of the tube.

of this droplet, and a flash with an ultraviolet lightbulb would polymerize the droplet, thus stabilizing it. However, this changes the molecular makeup of the droplet and does not give any understanding as to the underlying mechanics of the system. Perhaps we can supply a force as a counterbalance against surface tension to stabilize the droplet? This is where our experiments lie.

As Taylor demonstrated, electric fields do influence the breakup phenomena of droplets, yet his experiments occur over very short time scales. Current theories describing the effects of electric fields on the breakup of droplets assume an equipotential surface, but don't match the reality of the experiments due to the dynamics of the system [6]. To test the theory, we set our experiments apart by slowing down the dynamics of the system to achieve an equipotential surface, rather than trying to simulate the effects of a system out of electrical equilibrium. We do this by decreasing the surface tension by orders of magnitude via surfactants in both the inner and outer liquids. This increases the characteristic lifetime of the droplet, giving the charge a substantial amount of time to equilibrate on the surface. In the inner liquid, we use water with sodium dodecyl sulfate (SDS), which lets the water act as a conductor and decreases the surface tension by an order of magnitude. In the outer liquid, we introduce another surfactant called aminopropyl terminated silicon oil (ATSO), which also decreases the surface tension by an order of magnitude. Each of these decrease surface tension by an order of magnitude, and we are able to verify this by using the pendant drop method [7].

As the surface tension of the system decreases, the timescale associated with the break up does as well. Slowing down the dynamics of the system result in the droplet appearing to be stable for a longer period of time and lengthening all relevant time scales, except for charge equilibration time, which is not dependent on surface tension.

Calculations have predicted the following behavior: due to the geometry of the droplet, the charge distribution will be asymmetric. Gaussian curvature is the product of the two principle curvatures. One principle curve follows the inner circle that makes up the hole in the middle of the toroid, and this curvature is negative. The other principle curvature is perpendicular to that, bounding the circular cross section of the tube; this curvature is positive. Curvature is inversely proportional to the radius of the circle bounded by the curve, so the magnitude of the Gaussian curvature closer to the hole in the middle of the toroid (the handle) is high, and the magnitude of the Gaussian curvature on the outside of the toroid is low. See Fig. 2.2 for a visualization of this. Because the surface charge density is directly proportional to the magnitude of the Gaussian curvature, the charge density is much higher near the axis of revolution, and the electric field is much stronger there. This results in an uneven distribution of stresses, leading to a force pushing the toroid outwards theory on the mechanism by which instabilities are developed still needs more work.

Yet another method by which these droplets could be stabilized is the 3D printing of the droplets in a yield stress material. A yield stress material is one in which the material parameters change with the state of motion of the material itself. An example of this is a solution of corn starch and water. This behaves as a liquid when gently disturbed, but when subject to a shock force such as a slap or a punch, it behaves as a solid this is called

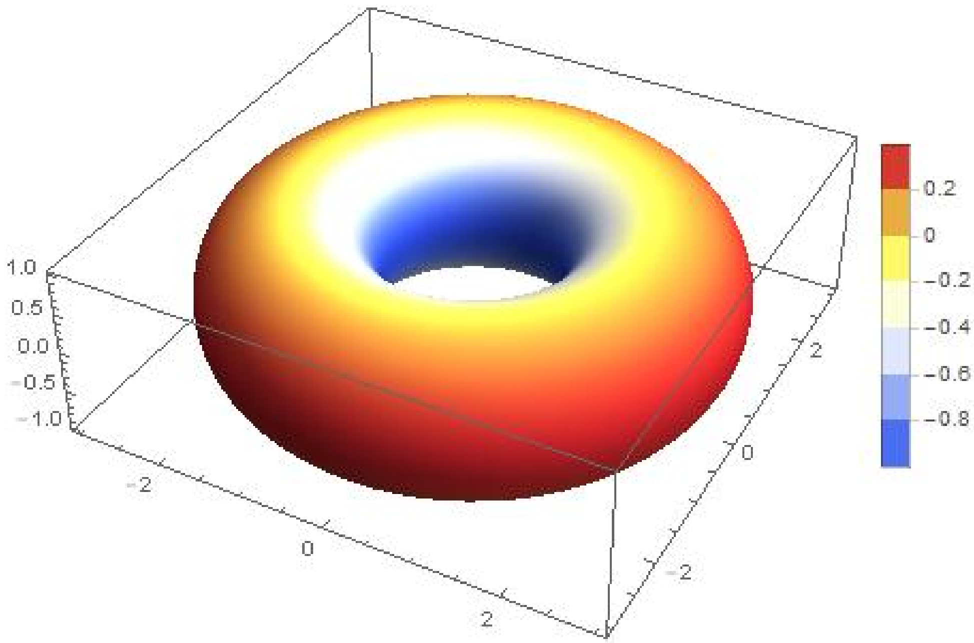

Figure 2.2: Gaussian curvature on a torus in three dimensional space. Surface charge density is directly proportional to the magnitude of the Gaussian curvature.

a shear thickening material and is due to the structure of the mixture on a molecular level. We are interested in a shear thinning material that behaves as a liquid while sheared. As we drag a needle through the material, the local area is sheared, enabling injection of the inner liquid, but the surrounding material comes to rest before the injected liquid has had a chance to deform [8]. We use a polymer called Carbopol ETD 2020 for our experiments, as it has a very high visibility [9].

Much of what has been discussed so far is concerned with the experimental setup and basis of how we will go about the experiments, but we are extremely concerned with the breakup mechanisms that emerge at sufficiently high voltage. The emergence of these viscous fingers is not regularly seen in a 3D non-porous media, and never induced by non-mechanical forces [10]. If these are indeed Saffman-Taylor Instabilities, any deeper understanding that we can acquire is extremely valuable.

CHAPTER 3

METHODS AND MATERIALS

3.1 Toroidal Droplet Instabilities

Before an understanding of the devolution and break-ups of droplets can be understood, there must first be an explanation of what makes a toroid unstable and how we go about generating the toroidal droplets. We can choose to describe a surface as a two-dimensional space where there is an interface between two different types of materials. For example, an interface between oil and water exhibits many interesting properties that are related to surface tension [11].

A useful lens through which we can examine surface tension utilizes dimensional analysis. Surface tension has units of $Pa \cdot m$, that is Pascal meters. By using the following equivalences, we can alter the way we look at surface tension:

$$Pa \cdot m = \frac{N \cdot m}{m^2} = \frac{J}{m^2}$$

Thus, surface tension can be examined as a surface energy density, or an energy cost per unit surface area in the units of Joules per meter^2. Therefore, if surface tension is specified, a given volume of a liquid will minimize its surface area in an attempt to minimize surface free energy in equilibrium. Droplets tend towards spherical shapes because a sphere is the minimal amount of surface area for a given volume [11].

3.2 Generation of Toroidal Droplets in Low Surface Tension Environments

Something of vital importance to our experimental set-up is the generation of toroids with long lifetimes. We wish to conduct experiments under these conditions so that electric charge is able to completely equilibrate on the surface of the torus, rather than observing the torus behavior in response to eddy-currents throughout the bulk and surface on the path to complete equilibration. Our approach to solve this problem involves minimizing the surface tension between our inner fluid and outer fluid.

In all experiments, the outer environment is an extremely high viscosity silicone oil. We choose a 30,000 cSt silicone oil sample with a surfactant mixed into it. The surfactant is aminopropyl-terminated silicone oil (ATSO) which serves the function of lowering the surface tension of generic silicone oil by an order of magnitude. The inner fluid is always less viscous in the outer, and we use a variety of materials. To start, we used a solution of deionized water and a salt called sodium dodecyl sulphate (SDS). The purpose of the salt is two-fold. On one hand, SDS acts as an electrolyte, turning the water from a complete electric insulator into a very effective conductor. Additionally, the SDS serves as a surfactant, once again decreasing the surface tension by an order of magnitude.

Our final experimental set-up involves a rectangular cuvette made of plexiglass sitting on a rotating stage. By activating a voltage source connected to an engine, we rotate the stage at a controlled velocity, and thus rotate the bath of silicone oil. As the bath rotates, we inject the inner fluid into the rotating environment via a metallic needle and a syringe pump. In a non-rotating environment, this would result in a cylindrical jet, but the rotation forces the jet to take on a constant curvature, resulting in a ring of finite thickness this is the toroid. Via a hole in the bottom of the rotating stage, we record the evolution of the torus from generation to eventual break-up. By using the video capture software IC Capture and image analysis software Image J, we take images at controlled intervals, as

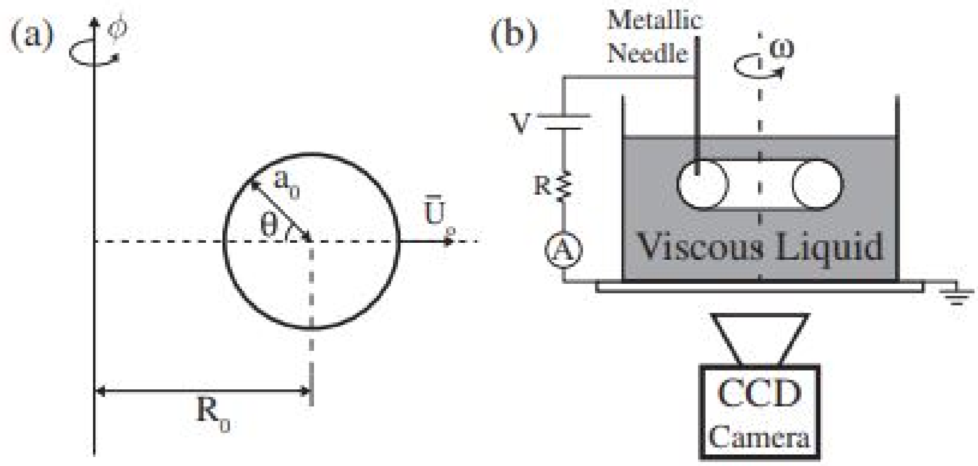

Figure 3.1: (a) Schematic of the circular cross section of a torus. R0 is the radius of the central circle, a0 is the tube radius, and is the polar angle. The torus is obtained by revolving this cross section along the direction. The velocity at = is radially outwards and has magnitude U0. (b) Schematic of the experimental setup. A bath containing silicone oil rotates with an angular speed of approximately 0.25 rad/s while the inner liquid is injected. The resultant toroidal droplet is charged at a voltage V. The subsequence evolution is captured using a CCD camera. [3]

well as conduct measurements, compare timescales, and quantitatively describe experiments [9]. For a visualization fo the geometry of a torus and a schematic of our experimental set up, see Fig. 3.1.

3.3 Application of Charge

Once the toroid has been formed, we activate a voltage source in contact with the metallic needle which is in contact with the toroid, thus transferring charge to maintain a voltage difference between the toroid and the metallic stage. This charge introduces another competing force, one due to electrostatic interaction.

Whereas the surface tension is a mechanically induced energy cost per unit area, the charges on the surface of the toroid also exert repulsive forces against one another. The applied voltage is a function of total charge on the torus, and it is an inherent characteristic in any conductor that the charge lies on the surface. Therefore, the charge will be distributed along the surface of the toroid, and as the surface area increases, the charge density decreases. The electrostatic repulsion that the torus feels is a function of charge density, therefore the repulsive energy due to the charges can also be looked at as an energy per unit area [3].

The difference in surface tension and electric stress lies in their signs. Surface tension tends to minimize the surface area to minimize the energy cost, yet electric stresses ideally maximize the surface area to minimize the repulsive energy. The resulting behavior is a competition between the surface tension and electric stresses.

3.4 Viscosity Reversal

One of the defining characteristics of the Saffman-Taylor Instability as demonstrated by Saffman and Taylor is that it only occurs when a more viscous fluid is displaced by a less viscous fluid. In our experiments, the outer fluid was always many orders of magnitude more viscous than the inner fluid. In an attempt to test whether or not the instability we observed actually was the Saffman-Taylor Instability, we had to rethink the experimental parameters of our system and attempt to generate the same experiment with a more viscous fluid displacing a less viscous one [5].

The first thing we needed to require is that the fluids must be immiscible. If the fluids were miscible, then we would not be able to generate a torus with meaningful geometries, if at all. With miscible fluids, the inner fluid would diffuse throughout the outer fluid on a molecular level over the course of our experiment, contaminating the outer fluid for subsequent experiments, as well as only giving results that are impossible to interpret for our purposes. To account for this, we concluded that silicone oil was an extremely viable candidate for the outer fluid, as silicone oil is insoluble in lubricating oils, fatty acids, animal and vegetable oils, water, and a number of organic solvents [12].

Of course, the inner fluid must also be more viscous than the outer fluid. Sigma-Aldrich carries silicone oils of viscosities as low as 5 cSt, so while we had a wide range of candidates for the outer fluid, we were still unsure about what to use for the inner fluid.

A third thing we had to consider was the density matching of the inner fluid and the outer fluid. If the inner fluid has a density of ρ_{in} and the outer fluid has a density of ρ_{out}, then we can define the density difference as $\Delta\rho = \rho_{in} - \rho_{out}$. When submerged in the outer fluid, not subject to any other lifting or sinking forces, the inner fluid adopts $\Delta\rho$ as its effective density. This leads to buoyant force on the inner fluid described by

$$F_B = V \cdot (\Delta\rho) \cdot g$$

where g is gravitational acceleration, $\ddot{z}$. If the inner fluid is more dense than the outer, that is $(\Delta\rho) > 0$, then this force pulls the inner fluid down, in the direction of gravity. However, if $(\Delta\rho) < 0$, the force pushes the inner fluid up until a sufficiently smaller amount of volume is occupied by the inner fluid.

For a given time t, we can approximate how far the inner fluid would fall. Note that in this scenario, drag forces are not important in the early stages of this estimation.

$$F = V \cdot (\rho_{in}) \cdot \ddot{z}$$

$$F \cdot (t - t_0) = V \cdot (\rho_{in}) \cdot \dot{z}$$

$$\text{Imposing } t_0 = 0$$

$$F\frac{t^2}{2} = V \cdot (\rho_{in}) \cdot (z - z_0)$$

$$z - z_0 = \frac{F \cdot t^2}{2V \cdot (\rho_{in})}$$

$$\text{Imposing } z_0 = 0 \text{ and } F = F_B$$

$$z = \frac{\Delta\rho \cdot g \cdot t^2}{2\rho_{in}}$$

So, for example, if ρ_{out} is $0.95 \cdot \rho_{in}$, then $\Delta\rho = 0.05\rho_{in}$. If we assume that $g = 10$ m/s^2, then the distance that the inner fluid has fallen a half second is $z = 0.25$ m = 25 cm. Due to the fact that we are constructing toroids with tube radii of approximately 2 mm, this much error is extremely problematic, so we must take care to density match the inner and outer fluids to great accuracy. Drag forces certainly will reduce the amount that the inner fluid moves, but this estimate demonstrates the importance of sedimentation effects.

Finally, our candidate must be conductive such that it can actually hold the charge on its surface. This is a necessity because otherwise, the surface charge density would not be high enough to have any effect on the system. So if we can find a fluid with a density between 940 and 1000 kg/m^3 that is immiscible in silicone oil, is more viscous than 5 cSt, and is an effective conductor, it is a viable candidate. Ultimately, we decided on castor oil with a mixture of 4% Span 80 to lower the surface tension and add conductivity. The castor oil has a viscosity of 650 cSt, and a density of .961 g/cm^3.

When we attempted to generate toroids in this viscosity contrasted environment, we first encountered issues with wrapping the jet around and coalescing onto itself. If generated in the same way as the water toroids, a spiral was formed that tightened with

Figure 3.2: Attempt of generation of castor oil torus within low viscosity silicone oil, during rotation. Notice how there is not a single torus, but a curved jet exhibiting higher curvature as the radius decreases.

every subsequent rotation, and a smooth jet was never generated (see Fig. 3.2). Our solution consisted of bending the needle to supply a radial velocity to the pumped liquid and counteract its tendency to immediately shrink (see Fig. 3.3).

This supplied a little more stability and let us generate toroids, but the toroids were shrinking rapidly. Before the volume had finished being pumped, the torus had shrank substantially from its initial radius, so there was no ”torus” to speak of. To fix this problem, we decided to move the needle in with the torus as the fluid was being pumped. As the radius of the ring got smaller, we manually shifted the needle in the antiradial direction such that the fluid was pumped along the torus. This is discussed further in the results section.

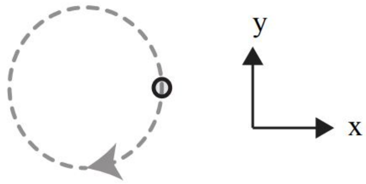

(a) Schematic of the bottom view of an unbent needle. The black circle represents the opening of the needle.

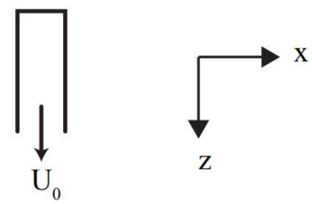

(b) Side view of an unbent needle. Pushes fluids in the positive z-direction.

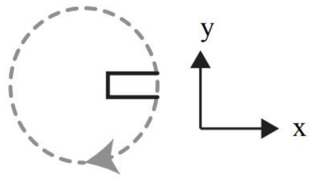

(c) Bottom view of a bent needle. Traces the same trajectory as (a). The open end of the rectangle represents the opening of the needle.

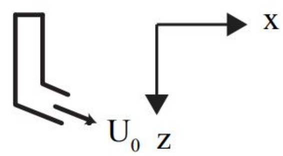

(d) Side view of a bent needle. Pushes fluid both in the positive z-direction and in the radial direction to prevent the shrinking effect.

Figure 3.3: Different views of needle orientation with respect to trajectory. In (a) and (c), the grey circle represents the trajectory of the needle. The arrow represents the direction of motion. In (b) and (d), U_0 represents the initial velocity of the inner fluid as it is pumped into the outer fluid. Note that in (d), this differs from our experimental apparatus in that our bend is smooth to avoid breaking the metal needle. In (a)-(d), positive z represents the direction of the gravitational force.

3.5 Automation of Generation

A secondary focus of this project was the ability to automate the generation of toroids and other unstable droplets. Alberto Fernandez-Nieves Soft Condensed Matter Lab at Georgia Tech co-owns two patents with Thomas Angelinis Soft Matter Lab at the University of Florida on a proprietary method of three-dimensional printing involving the usage of viscoelastic materials and their properties.

A viscoelastic material is a material that utilizes viscous characteristics of liquids and the elastic characteristics of solids, and by manipulating the dual behavior of these materials, we can stabilize a wide variety of figures. The main material that I am focused on is a polymer gel named Carbopol ETD 2020 due to its visibility and viscoelastic properties at a neutral pH. These characteristics in turn make Carbopol ideal for observation of unstable shapes.

At rest, the material is a solid. It does not flow, demonstrates elastic behavior in that it will return to its original shape if sheared slightly. However, if sheared hard enough, Carbopol will behave as a liquid. It exhibits viscous behavior in that it flows, and it does not return to its original shape. By strategically shearing Carbopol and injecting fluid into the area being sheared, we can print our choice of shapes [13]. As the sheared areas are left alone, they begin to behave as solids again, offering a counteractive force against any deformation the injected fluid attempts to take on. Effectively, the elasticity of the viscoelastic material resists the tendency for droplets surface tension to force to force the droplets into spheres, stabilizing the droplets in their unstable geometries.

With regards to this method specifically, were not able to make progress in quantitatively describing the parameter space in which this three-dimensional printing method is effective with Carbopol ETD 2020. Among other variables, the parameter space includes variables such as flow rate, needle velocity, needle width, and concentration of Carbopol.

CHAPTER 4

RESULTS

Figure 4.1 demonstrates the different behavior that we observe when different electric voltages are applied. In image (a), the outer ring of the torus is highlighted with a white dashed line. The radial velocity of this ring is denoted by U_0. As is shown in subsequent photos, U_0 increases with voltage. In image (k), we can see the emergence of the fingers in their beginning stages. In image (l), we see the fingers fully developed, penetrating into the outer medium. Due to the low surface tension present in our system, the evolutions of these droplets take place over the course of minutes, not seconds. This ensures that the charge given by the needle equilibrates on the surface before breakup is observed.

Figure 4.2 shows the evolution of a viscosity inverted system in which we generated a torus of castor oil in a 600 cSt silicone oil environment. While we did see massive distortion of the torus in response to the application of charge via the battery, it was not the viscous fingering that we saw in the previous situation. Upon the application of a voltage of 2200 V, there was a violent response during which the torus ejected droplets at high velocity into the silicone oil. This was followed by the torus expanding, twisting, and ejecting jets into the silicone oil. We never observed a breakup similar to the ones seen in Fig. 4.1.(f,i,k,l). Our explanation of this break up is that the surface of the castor oil torus was supersaturated with charges, and the ejection of droplets or sharp jets was simply the favored method of charge ejection.

This secondary experiment that consisted of disproving other possible explanations not only reaffirmed our confidence that the instability we observed was the Saffman-Taylor Instability, but actually demonstrated other ways to troubleshoot problems in toroid generation. Up to this point, we had not generated toroids with a bent needle, nor moved

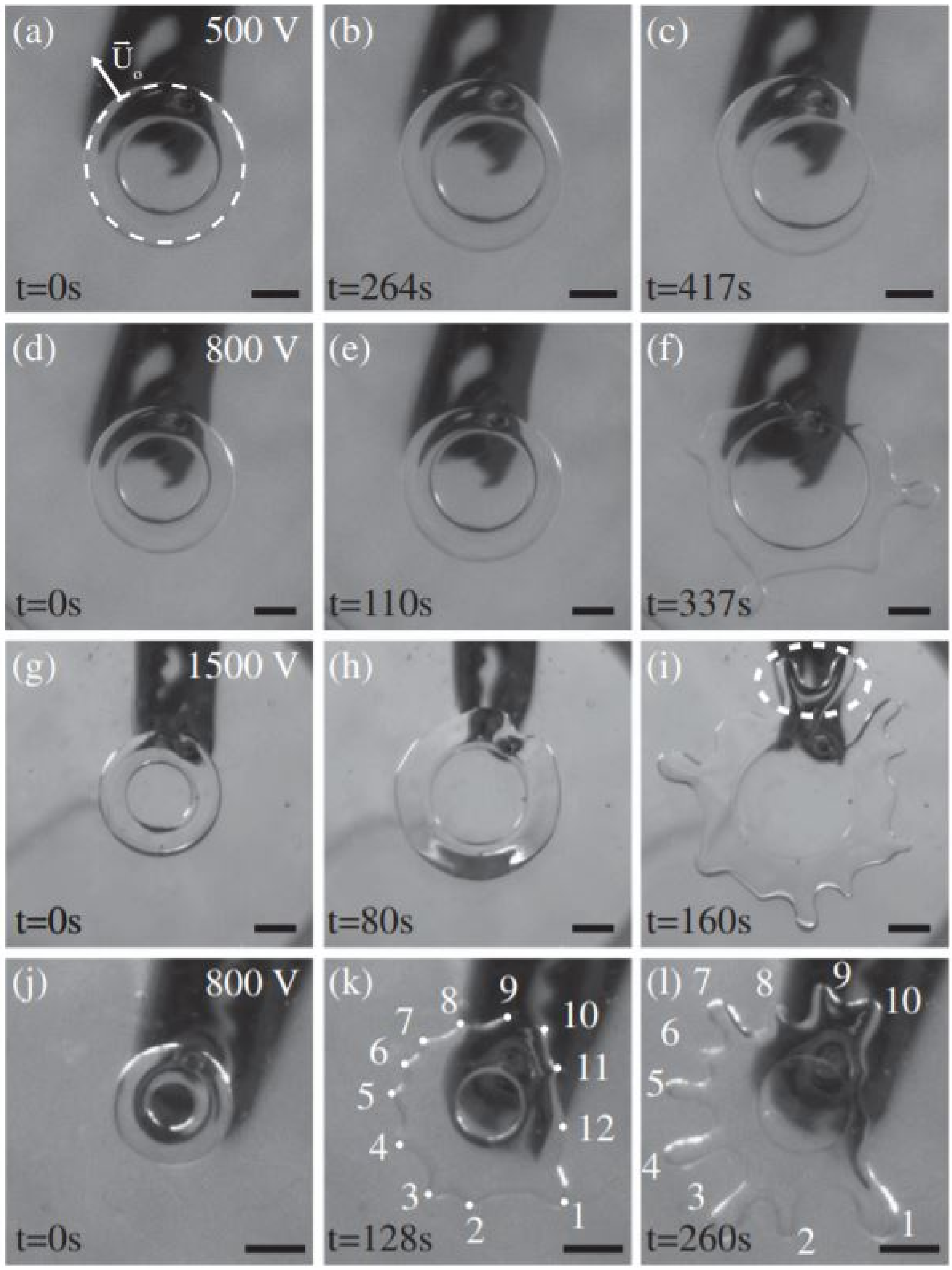

Figure 4.1: This figure shows the range of behavior charged toroidal droplets over various time scales and various voltages. Notice that not every application of voltage results in the fingering breakup. In frames (a)-(c), 500 V are applied, and fingering breakup is not observed.

the needle to accommodate unpredictable motion of the torus. In other experiments, we found that actually applying charge during the toroid generation gave short term stability, but we were not able to extract any meaningful data from those experiments.

Ultimately, we were able to classify the state of the torus upon breakup into one of five separate bins. These bins are as follows: shrink, shrink/expand, expansion, expand/finger, and viscous fingering. We classify breakup as the moment at which we can no longer take a valid measurement of the torus characteristics, whether that is because of distortions along the circumference or collapse into a sphere. Our phase map is shown in Figure 4.3.

The phase map plots the capillary number Ca vs. the aspect ratio R_0/a_0. The definition of the capillary number is the ratio of the viscous stresses to the surface tension given by

$$Ca = \frac{\mu U_0}{\gamma}$$

where μ is the viscosity of the outer medium, U_0 is the velocity of the interface, and γ is the surface tension. Interestingly enough, viscous fingering was always seen at a capillary number greater than 0.4.

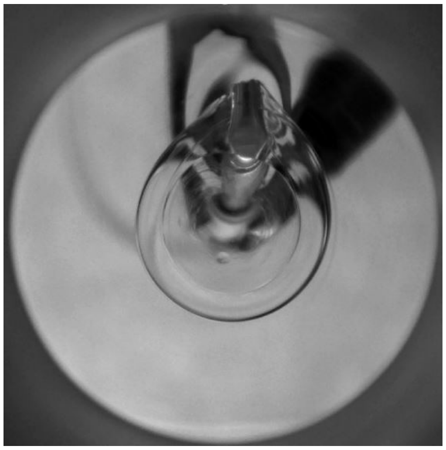

(a) A torus generated with a bent needle that has not been moved to accommodate the shrinking ring. This is before the volume has finished being pumped. Notice how the opening of the needle is not even in contact with the ring.

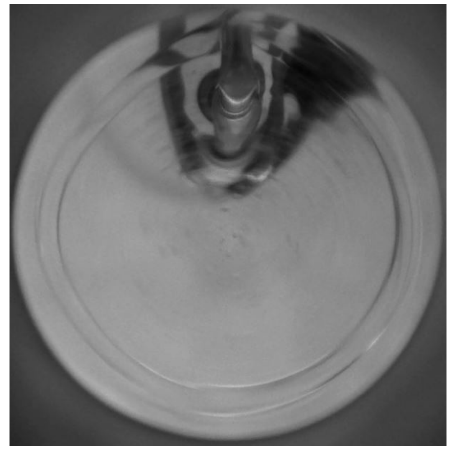

(b) The starting position of the needle after one rotation has already been completed. Note that this is not the same trial as (a), and this picture depicts the experiment as the cuvette is rotating.

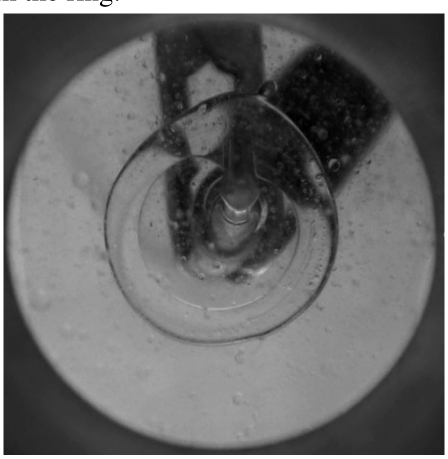

(c) The final position of the needle from (b). Notice how the opening of the needle is well within the torus.

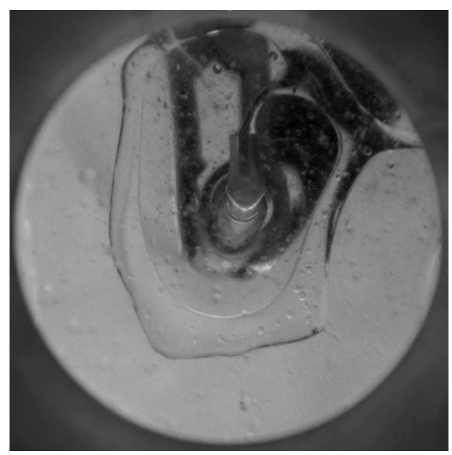

(d) The reaction of the torus from (b) and (c) to the application of 2200 V.

Figure 4.2: Castor oil toroids generated in 600 cSt silicone oil. Even when the inner fluid had a radical reaction to the application of a high voltage, we did not observe the Saffman-Taylor instability.

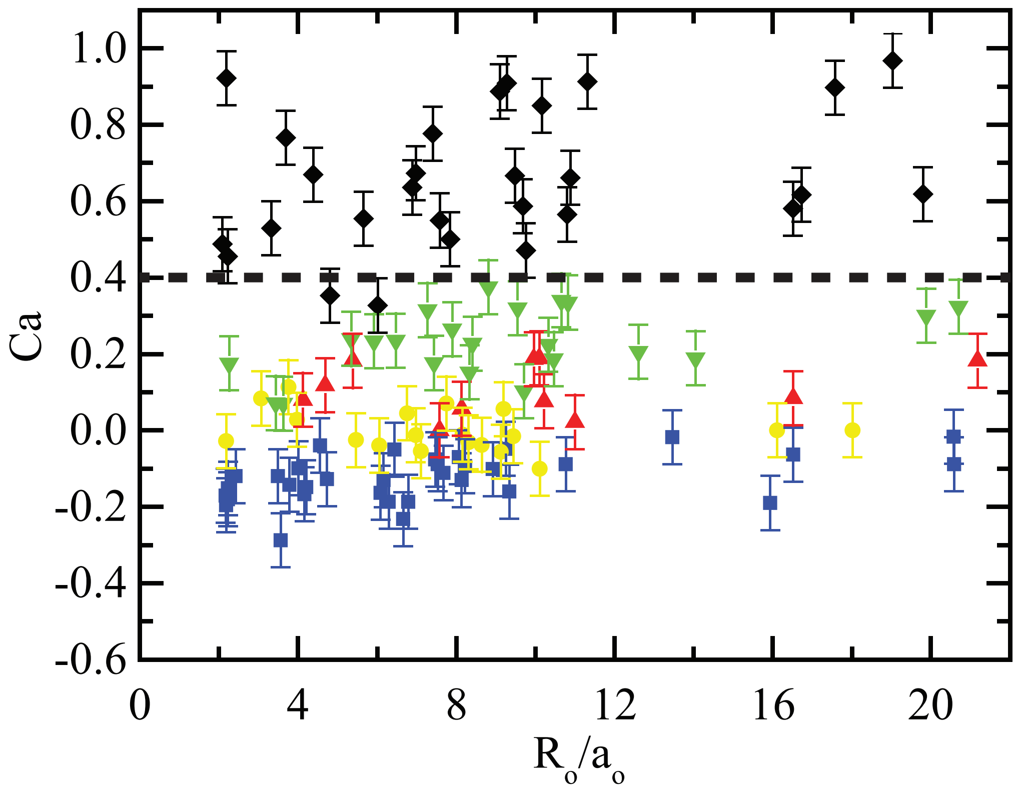

Figure 4.3: Phase map of the breakup of the torus in the capillary number vs. aspect ratio space. The blue squares represent toroids that fell within the shrinking bin. The yellow diamonds represent toroids that fell within the shrink/expand transition bin. The red triangles represent toroids that fell within the expansion bin. Green inverted triangles represent toroids that fell within the expand/finger transition bin. Black diamonds represent toroids that clearly exhibited viscous fingering.

CHAPTER 5

DISCUSSION

In our experiment, there were two dominating forms of breakup. The first, which results when the imposed voltage is 0 for a sufficiently thin torus, is the Rayleigh-Plateau Instability. This is also called jet breakup. There is a characteristic time-scale associated with this break up of

$$t_{R-P} \approx \frac{2\mu a_0}{\gamma}$$

In this situation, μ is once again the viscosity of the outer medium, a_0 is the tube radius of the torus, and γ is the surface tension [1].

The second dominating form of breakup is the Saffman-Taylor Instability. This is referred to as viscous fingering, and it has a characteristic time-scale associated with it of

$$t_{S-T} \approx \frac{a_0}{U_0}$$

In this situation, U_0 is the magnitude of the velocity of the outer ring of the torus [14]. We choose to view the dominant breakup of the system as the winner of a competition between these two breakup mechanisms, and whichever has the shorter characteristic timescale dominates the mode of breakup. That is, if

$$t_{S-T} < t_{R-P}$$

the Saffman-Taylor Instability will dominate.

Our observation of the emergence of the Saffman-Taylor Instability has important implications for both topological mathematical systems and physical theories governing unstable droplets breakup. With respect the mathematical systems, the mathematical approach we use breaks the cylindrical symmetry of the problem and instead reduces the system to a two-dimensional non-equilibrium situation.

Physically, however, the system is novel for many reasons. The geometry of the situation results in an asymmetric charge distribution which, in turn, causes a force imbalance. This force imbalance causes a mechanical shift in the structure of the droplet, which enables the formation of fingers. Therefore, not only have we shown that the Saffman-Taylor Instability can exist in three-dimensional environments, but it can also be induced by forces other than mechanical ones. In this case, the electrostatic stress induces the instability.

Additionally, in the search for proof that this was the Saffman-Taylor instability, we discovered that there are many ways to account for the various problems that evidence themselves in the production of energetically unfavorable droplets. Specifically, we dealt with the trials of generating high viscosity droplets in a low viscosity environment. We discovered that altering the direction that the fluid is pumped, as well as shifting the injection needle with the produced jet does allow us to produce droplets that would otherwise not be possible.

REFERENCES

[1] S. Tomotika, “On the instability of a cylindrical thread of a viscous liquid surrounded by another viscous fluid,” *Proceedings of the Royal Society of London. Series A - Mathematical and Physical Sciences*, vol. 150, no. 870, pp. 322–337, 1935.

[2] A. A. Fragkopoulos, E. Pairam, E. Berger, P. N. Segre, and A. Fernndez-Nieves, “Shrinking instability of toroidal droplets,” *Proceedings of the National Academy of Sciences*, vol. 114, no. 11, pp. 2871–2875, 2017.

[3] A. A. Fragkopoulos and A. Fernandez-Nieves, “Toroidal-droplet instabilities in the presence of charge,” *Physical Review E*, vol. 95, no. 3, p. 033 122, 2017.

[4] G. Taylor, “Disintegration of water drops in an electric field,” *Proceedings of the Royal Society of London. Series A. Mathematical and Physical Sciences*, vol. 280, no. 1382, pp. 383–397, 1964.

[5] S. G. T. P. G. Saffman, “The penetration of a fluid into a porous medium or hele-shaw cell containing a more viscous liquid,” *Proceedings of the Royal Society of London. Series A. Mathematical and Physical Sciences*, vol. 245, no. 1242, pp. 312–329, 1958.

[6] E. Pairam, J. Vallamkondu, V. Koning, B. C. van Zuiden, P. W. Ellis, M. A. Bates, V. Vitelli, and A. Fernandez-Nieves, “Stable nematic droplets with handles,” *Proceedings of the National Academy of Sciences*, vol. 110, no. 23, pp. 9295–9300, 2013.

[7] E. Y. Arashiro and N. R. Demarquette, “Use of the pendant drop method to measure interfacial tension between molten polymers,” *Materials Research*, vol. 2, no. 1, pp. 23–32, 1999.

[8] T. Bhattacharjee, S. M. Zehnder, K. G. Rowe, S. Jain, R. M. Nixon, W. G. Sawyer, and T. E. Angelini, “Writing in the granular gel medium,” *Science advances*, vol. 1, no. 8, e1500655, 2015.

[9] E. Pairam and A. Fernandez-Nieves, “Generation and stability of toroidal droplets in a viscous liquid,” *Physical Review Letters*, vol. 102, no. 23, p. 234 501, 2009.

[10] R. A. L. Jones, *Soft condensed matter*. Oxford; New York: Oxford University Press, 2002, ISBN: 0198505906 9780198505907 0198505892 9780198505891.

[11] A. M. P. Alberto Fernandez-Nieves, *Fluids, Colloids, and Soft Materials: An Introduction to Soft Matter Physics*, 1st, ser. Surface and Interfacial Chemistry. Wiley, 2016, p. 432, ISBN: 978-1118065624.

[12] Web Page, 2015.

[13] E Pairam, H Le, and A Fernndez-Nieves, "Stability of toroidal droplets inside yield stress materials," *Physical Review E*, vol. 90, no. 2, p. 021 002, 2014.

[14] L. Paterson, *J. Fluid Mech*, vol. 113, no. 513, 1981.